



**HAL**  
open science

## Eco-designed Conformable Inorganic Electronics to Improve the End of Life of Smart Objects: Sensor Processing and Applications

Maxime Harnois, Fatima Garcia-Castro, Gaëtan Herry, Olivier De Sagazan,  
France Le Bihan

### ► To cite this version:

Maxime Harnois, Fatima Garcia-Castro, Gaëtan Herry, Olivier De Sagazan, France Le Bihan. Eco-designed Conformable Inorganic Electronics to Improve the End of Life of Smart Objects: Sensor Processing and Applications. *ACS Applied Electronic Materials*, 2020, 2 (2), pp.563-570. 10.1021/ac-saelm.9b00807 . hal-02651031

**HAL Id: hal-02651031**

**<https://univ-rennes.hal.science/hal-02651031>**

Submitted on 4 Jun 2020

**HAL** is a multi-disciplinary open access archive for the deposit and dissemination of scientific research documents, whether they are published or not. The documents may come from teaching and research institutions in France or abroad, or from public or private research centers.

L'archive ouverte pluridisciplinaire **HAL**, est destinée au dépôt et à la diffusion de documents scientifiques de niveau recherche, publiés ou non, émanant des établissements d'enseignement et de recherche français ou étrangers, des laboratoires publics ou privés.

1  
2  
3  
4  
5  
6  
7 Eco-designed conformable Inorganic Electronics to  
8  
9  
10  
11 Improve the Smart Object End of Life: sensor's  
12  
13  
14  
15 processing and applications.  
16  
17  
18  
19

20 *Maxime Harnois\**, *Fatima Garcia Castro*, *Gaëtan Herry*, *Olivier De Sagazan*, *France Le Bihan*  
21  
22

23  
24  
25  
26  
27 Université Rennes 1, Institut d'Électronique et des Télécommunications de Rennes,  
28

29  
30 UMR CNRS 6164, Département Microélectronique & Microcapteurs, Campus de  
31

32  
33  
34 Beaulieu, 35042 Rennes Cedex, France  
35  
36

37  
38  
39 KEYWORDS: Inorganic strain sensors; Conformable Electronics; Water Soluble  
40

41  
42 Electronics; WEEE Standard; Ecodesigned Electronics.  
43  
44

45  
46 ABSTRACT.  
47

48 The plastic pollution is indisputable and technologies aiming to add flexible electronics onto  
49 objects have to take into consideration such environmental issue. Faced with this challenge, the  
50 development of technologies that comply with current standards such as WEEE (Waste Electric  
51 and Electronic Equipment) legislation is crucial. Green electronics based on fully biodegradable  
52  
53  
54  
55  
56  
57  
58  
59  
60

1  
2  
3 materials is under development but needs time to be put on the market. Meanwhile, inorganic  
4 electronic remains a good candidate. Consequently, it makes sense to transfer inorganic electronics  
5 onto objects before it dismantling and recoveries.  
6  
7

8  
9  
10 Here, an eco-designed technology allowing the transfer of electronics onto objects is detailed.  
11 Silicon-based devices are transferred from polyimide substrate (PI) to water-soluble substrate  
12 (PVA: Poly(vinyl alcohol)). It is highlighted that the transfer of inorganic layers from PI to PVA  
13 substrate does not have a negative impact on the devices mechanical and electrical characteristics.  
14  
15 To demonstrate such concept, strain gauges and temperature sensors have been transferred onto  
16 daily life object reaching the same performances than sensors fabricated onto polyimide substrate.  
17  
18 Moreover, materials transferred onto the object using PVA substrate can be dismantled and  
19 recovered at the end of object's life highlighting that hydrosoluble substrate is a good candidate  
20 towards an eco-designed technology.  
21  
22  
23  
24  
25  
26  
27  
28  
29  
30  
31  
32  
33

### 34 **1. Introduction**

35  
36 High-tech products are becoming essential in our daily life promoting a constant growth  
37 of the electronic industry. Thus, the everyday objects are smarter and smarter as  
38 embedded electronics giving them extra functionalities.<sup>1</sup> However, our new consumption  
39 needs must not be done, once again, at the expense of the environment. Faced with this  
40 challenge, Extended Producer Responsibility (EPR) principle has been established by the  
41  
42  
43  
44  
45  
46  
47  
48  
49  
50  
51  
52  
53  
54 Organization for Economic Cooperation and Development (OECD).<sup>2</sup> This is a cornerstone  
55  
56  
57  
58  
59  
60

1  
2  
3 principle of waste prevention and reduction policy. The basic idea of EPR is to hold  
4  
5  
6  
7 producers responsible for the environmental impact of their products at the end of life  
8  
9  
10 pushing them to change their practices towards the eco-design (also called design for  
11  
12  
13 environment activities) and the respect of the Waste Electric and Electronic Equipment  
14  
15  
16 (WEEE) legislation (Directive 2002/96/EC of the European Parliament and of the  
17  
18  
19 Council).<sup>3,4</sup> Consequently, eco-designed fabrication processes taking into consideration  
20  
21  
22 the smart object end of life should be developed to respect the WEEE legislation. Up to  
23  
24  
25 know, this aspect is overlooked in works dealing with novel technologies development  
26  
27  
28 especially in the field of new generation of electronics such as “plastic electronics”.  
29  
30  
31  
32  
33

34  
35 In the near future, connected objects will embed sensors,<sup>5,6</sup> displays,<sup>7,8</sup> photovoltaic  
36  
37  
38 panels,<sup>9,10</sup> antennas,<sup>11,12</sup> etc. not only into but also at the surface of the object. Among  
39  
40  
41 technologies developed to intimately wrap electronics onto 3D objects, those using  
42  
43  
44 polymeric substrates (flexible or even stretchable) are frequently reported. This last 15  
45  
46  
47 years, research has focused on materials and methods to improve devices performances  
48  
49  
50 and conformability instead of environmental concerns or even circular economy. Indeed,  
51  
52  
53  
54  
55  
56  
57  
58  
59  
60



1  
2  
3 original concepts have been developed such as ultrathin electronics,<sup>9,13</sup> stretchable  
4  
5  
6  
7 electronics<sup>14–17</sup> or even thermoforming technologies.<sup>18</sup> However, polymeric substrates  
8  
9  
10 (e.g., polyimide: PI, Polyethylene terephthalate: PET, Polyethylene naphthalate: PEN,  
11  
12  
13 parylene, polydimethylsiloxane: PDMS ...) are permanently stuck onto the 3D object that  
14  
15  
16  
17 negatively impact Electric and Electronic Equipment (EEE) recycling.  
18  
19

20  
21 Recently, a number of biodegradable polymers, e.g. cellulose, chitin, silk, etc. have been  
22  
23  
24  
25 considered as substrates for environmental concerns or even for the fabrication of  
26  
27  
28 implantable electronics, piezoelectric energy harvester.<sup>19–23</sup> Biodegradable substrates  
29  
30  
31  
32 can lead to the same results in term of conformability than classical polymeric substrate  
33  
34  
35  
36 however they are not compatible with clean room processing (e.g., the photolithography  
37  
38  
39 or the wet etching steps). To overcome this challenge, novel fabrication methodologies  
40  
41  
42  
43 have to be developed.<sup>24</sup>  
44  
45

46  
47 Here, a comparative study between inorganic strain sensors fabricated onto polyimide substrate  
48  
49 and water soluble substrate is detailed. It will be shown that the process developed to transfer the  
50  
51 inorganic layer from PI to PVA substrate Poly(vinyl alcohol) did not have a negative impact on  
52  
53  
54 the devices electrical characteristics. Note that, the process described in this work cannot be  
55  
56 considered as eco-friendly because it meets all the perquisites of standard cleanroom  
57  
58  
59  
60

1  
2  
3 manufacturing (chemical etching, photolithography, etc.) and can be transferred to the industry  
4  
5 (contrary to green electronics, to date). However, the concept describes in the last section can be  
6  
7 considered as eco-designed because it will highlights that hydrosoluble substrate is a good  
8  
9 candidate facing smart object recycling issues because inorganic devices can be unmounted from  
10  
11 the object surface to be recovered.  
12  
13  
14  
15  
16

## 17 **2. Results and Discussion**

### 21 **a. Inorganic processing onto hydro-soluble substrate**

22  
23  
24 The figure 1 highlights the fabrication process of multilayered devices transferred onto a PVA  
25  
26 substrate. The process is fully compatible with cleanroom fabrication even if the targeted substrate  
27  
28 is water soluble. Experimental parameters are fully detailed in the experimental section. As shown  
29  
30 in figure 1a, at first, a PDMS layer was spin coated on a silicon carrier substrate and cured. A  
31  
32 25 $\mu\text{m}$  thick polyimide (PI) substrate was laminated onto the PDMS (figure 1b). The adhesion  
33  
34 forces between PDMS and PI are strong enough to provide a good sticking during the whole  
35  
36 process. The 3D scheme in the figure 1c shows that multilayered thin films can be deposited and  
37  
38 patterned at lithographical accuracy. Here, resistors made of two inorganic layers were fabricated.  
39  
40 Electrodes and resistive layers were made of aluminum and silicon, respectively. As shown in the  
41  
42 figure 1d, the PVA solution was spin coated following the protocol already described in a previous  
43  
44 work.<sup>17</sup> As a results, the inorganic devices were sandwiched between the PI and the PVA layers  
45  
46 (figure 1e). The total thickness of the structure was approximately equaled 55 $\mu\text{m}$  and was flexible.  
47  
48  
49  
50  
51  
52 The multilayered flexible substrate can be easily peeled off from the PDMS and flipped on it.  
53  
54  
55  
56  
57  
58  
59  
60 Thus, the PVA substrate adheres to the PDMS. Indeed, PDMS is well known to adheres to many

1  
2  
3 kind of surfaces as it is extensively used in microfluidics for instance.<sup>25</sup> Note that, the PDMS  
4 substrate can be reused from one process to another. The last stage consists in the dry etching of  
5 the PI films using O<sub>2</sub> plasma. After PI films fully-etching, the inorganic devices was transferred to  
6 the PVA substrate as shown in the 3D schemes of figure 1g and in the optical pictures of the figures  
7 1h and 1i.

8  
9  
10  
11  
12  
13  
14 The figure 1k highlights the time sequence of the PVA substrate dissolution. Note that, in the  
15 figure 1h, a PI ring remains after dry etching of the PI substrate. This etching residue is due to the  
16 mechanical clamp used to fix the wafer during the etching stage. The top left image of the figure  
17 1k highlights that a part of the flexible substrate is composed of a PVA film (transparent area) as  
18 substrate and a sandwich of PVA and PI (i.e., the dark yellow etching residue). In the figure 1k,  
19 after approximately 90 seconds, The PVA substrate was fully dissolved in water whereas the PI  
20 substrate was intact with inorganic material remaining on it. Consequently, the fabrication process  
21 does not damaged the PVA substrate and especially it ability to be dissolved in water.  
22  
23  
24  
25  
26  
27  
28  
29  
30  
31  
32  
33  
34  
35  
36  
37  
38  
39  
40  
41  
42  
43  
44  
45  
46  
47  
48  
49  
50  
51  
52  
53  
54  
55  
56  
57  
58  
59  
60

#### **b. Inorganic strain sensor**

Inorganic strain sensors were fabricated on two kinds of substrates: a 25 $\mu$ m thick  
Polyimide and a 30  $\mu$ m thick PVA substrate. As shown in Figure 2, their response to  
mechanical strain were analyzed in static (as function of bending radius) and dynamic

1  
2  
3 modes (voltage and resistivity as function of time and applied strain). In static mode  
4  
5  
6  
7 (figures 2a, 2b and 2c), the protocol consists in the measurement of the current as  
8  
9  
10 function of the voltage in the range of plus to minus 1V when substrate is flat (bending  
11  
12  
13 radius equals 0). It allows to determine the initial value of the resistivity. Then, the  
14  
15  
16 substrates were fixed to a tensile bending tools (half cylinders) and were bent from the  
17  
18  
19 lowest curvature (i.e., the lower applied strain) to the highest curvature (i.e., the highest  
20  
21  
22 applied strain). The bending radii were fixed to 0 (flat), 2.5 (R1), 2 (R2), 1.5 (R3) and 1  
23  
24  
25  
26  
27  
28 cm (R4).  
29  
30  
31

32 Then, the gauge factor (GF) is used to qualify the sensitivity of strain sensors fabricated  
33  
34  
35 onto the PVA and the PI substrate as shown in figures 2b and 2c, respectively. GF is  
36  
37  
38 defined by the Equation (1) as the ratio of the relative change of the sensors resistivity  
39  
40  
41  
42  
43 ( $\Delta R/R_0$ ) and the strain  $\epsilon$  applied to the sensor:  
44  
45  
46

$$GF = \frac{\Delta R}{R_0} \epsilon \quad (1)$$

47  
48  
49  
50  
51 For metals, GF is low, between 2 and 5<sup>26</sup> whereas for semiconductors such as silicon,  
52  
53  
54  
55 GF exhibits much larger values around 100 for single crystalline silicon (sc-Si), between  
56  
57  
58  
59  
60

1  
2  
3 20 and 40 for poly crystalline silicon (poly-Si) <sup>27</sup> or 20–30 for amorphous silicon (a-Si) <sup>28</sup>.  
4  
5  
6

7 In this work, microcrystalline silicon is deposited. The SG has already been determined  
8  
9  
10 in previous works and is fixed to 80GPa <sup>29</sup>. Here, the strain ( $\epsilon$ ) applied to the structure is  
11  
12  
13 function of the radius of curvature.  $\epsilon$  is calculated using the already proposed model for a  
14  
15  
16 bi-layer device taking into consideration their thicknesses and their Young modulus ( $Y$ ).<sup>29</sup>  
17  
18  
19

20  
21 In this work, the material properties and device structure are presented in the figure 1 and  
22  
23  
24 the Table S1 of the supporting information. This model takes into account the substrate  
25  
26  
27 and the stiffest layer (i.e. the silicon), which mainly define the mechanical behavior of the  
28  
29  
30 device. Consequently, the bilayer model is thus constituted by the PI substrate and the  
31  
32  
33 Si layer and the longitudinal strain  $\epsilon_{surface}$  applied on the surface of the layer is given by  
34  
35  
36  
37  
38  
39 the equation (2) derived from [25]:  
40  
41  
42  
43  
44  
45  
46

$$\epsilon_{surface} = \left( \frac{1}{r} \pm \frac{1}{r_0} \right) \left( \frac{d_s + d_f}{2} \right) \left( \frac{1 + 2\chi\eta + \chi\eta^2}{(1 + \eta)(1 + \chi\eta)} \right) \quad (2)$$

47  
48  
49  
50  
51  
52  
53  
54  
55  
56  
57  
58  
59  
60

1  
2  
3 where  $r$  and  $r_0$  are the applied and initial radii of curvature, respectively,  $d_s$  and  $d_f$  are  
4  
5  
6  
7 substrate and layer thicknesses, respectively, and are defined by  $\chi=Y_f/Y_s$  and  $\eta=d_f/d_s$ ,  
8  
9  
10 where  $Y_s$  and  $Y_f$  are substrate and layer Young moduli, respectively. The plus (or minus)  
11  
12  
13 signs depends on applied bending opposite to (or with) the built-in curvature. The silicon,  
14  
15  
16  
17 the PI and the PVA thicknesses were measured and were equaled 100nm, 25 $\mu$ m and  
18  
19  
20  
21 30 $\mu$ m, respectively. To calculate the strain, the young modulus of the PI and the PVA  
22  
23  
24 substrates have been fixed to 5GPa<sup>30</sup> and 1.9GPa, respectively, according to the  
25  
26  
27  
28 literature.<sup>16</sup>  
29  
30  
31

32  
33 Figures 2b and 2c show that SG values equal -21 and -24 for sensors fabricated onto  
34  
35  
36 PVA and PI, respectively. It can be notice that the collected data points (see in figure 2b)  
37  
38  
39 corresponding to the highest strain value has not been taken into consideration in the  
40  
41  
42 calculation of GF. Indeed, as shown in figure S1, when the strain exceeds approximately  
43  
44  
45  
46 0.14% cracks occur in the silicon layer leading to drastically increases the strain sensors  
47  
48  
49 resistivity. An option to decrease the strain is to reduce the substrate thickness ( $d_s$ ).  
50  
51  
52  
53 Indeed, as shown in figures 2b and 2d, at same radius of curvature, the applied strain in  
54  
55  
56  
57  
58  
59  
60

1  
2  
3  
4 PI is lower than the applied strain in PVA mainly because the PVA substrate was 5 $\mu$ m  
5  
6  
7 thicker than the PI substrates. However, it is demonstrated that the sensitivity and the  
8  
9  
10 mechanical behavior of the strain sensors is in the same order of magnitude proving that  
11  
12  
13  
14 the fabrication process does not impact the strain sensors response.  
15  
16  
17

18 As shown in the figures 2d, 2e and 2f, the strain sensors have been mounted onto a  
19  
20  
21 rubber based membrane submitted to a differential pressure (see also in the  
22  
23  
24 supplementary figure S2). Each 5 seconds, a pulse of 900 mbar is applied onto the  
25  
26  
27  
28 membrane that deforms the sensors (Elveflow pressure controller; MK3). The value of  
29  
30  
31  
32 the sensor resistivity is recorded, amplified and converted in voltage using analogic  
33  
34  
35  
36 circuits in combination with Arduino Uno development Kit.  
37  
38  
39

40 The variation of the voltage as function of time is plotted in the figures 2e and 2f. It  
41  
42  
43 highlights that whatever the substrate a signal can be recorded showing a good response  
44  
45  
46  
47 of the sensors in dynamic mode. Finally, sensors have been mounted onto the finger joint  
48  
49  
50  
51 of a nitrile glove. The variation of the resistivity as function of the finger motion is recorded  
52  
53  
54 and shown in the figures 2g, 2h and 2i. These experiments highlight that inorganic strain  
55  
56  
57  
58  
59  
60

1  
2  
3 gauge fabricated onto PVA substrate can be used as sensors for prosthetic hands has  
4  
5  
6  
7 already demonstrated for these fabricated onto other plastic substrates.<sup>31-33</sup> However, the  
8  
9  
10 main difference can rely on the WEEE management of such devices has demonstrated  
11  
12  
13  
14 in the next section.

### 18 **c. WEEE management**

19  
20 On the one hand, significant challenges in the management of WEEE are the dismantling  
21  
22  
23 and the recovery of materials.<sup>34</sup> On the other hand, it can be anticipated that most of our  
24  
25  
26  
27 future products will embed electronics. For instance, daily life objects such as a T-Shirt  
28  
29  
30 that will embed sensors or RFID Tag will be not considered as a T-shirt from recycling  
31  
32  
33  
34 point of view, but as a WEEE. Consequently, the objects' end of life must be taken into  
35  
36  
37  
38 consideration when a new technology is developed in order to respect the eco-design  
39  
40  
41  
42 rules already fixed by the legislation. It is the case of flexible electronics, the results  
43  
44  
45 detailed in the previous section and in the literature have demonstrated that plastic  
46  
47  
48 electronics can conformably wrap daily life object. However, the question of the EoL is  
49  
50  
51  
52 not taken into consideration. For instance, when plastic foils will be stuck onto the object,  
53  
54  
55  
56 can the electronics devices be separated easily from the object? Furthermore, when  
57  
58  
59  
60



1  
2  
3 devices are fabricated onto conventional plastics such as PI substrates, is device's  
4  
5  
6  
7 materials can be dismantled from the substrate? From recovery point of view, some of  
8  
9  
10 most interesting materials are metals. Is it possible to recovery the pure metals and reuse  
11  
12  
13 them as high grade electronics materials? In future works, these questions cannot be  
14  
15  
16  
17 avoid and need to be systematically taken into consideration.  
18  
19

20  
21  
22 This section highlights that the technology based on water soluble substrate to transfer  
23  
24  
25 inorganic devices onto daily life objects fits the requirement of the WEEE legislation as  
26  
27  
28 materials can be recovered. Moreover, the daily life object can be reused. To take benefit  
29  
30  
31 from PVA as sacrificial layer from WEEE recycling point of view, resistive inorganic  
32  
33  
34  
35 temperature sensors have been conformably wrapped onto a daily life object (a cup). The  
36  
37  
38 following experiments illustrate our concept and highlight how inorganic material can be  
39  
40  
41 recovered after the object lifecycle.  
42  
43  
44

45  
46  
47 The figures 3a, 3b and 3c show the daily life object (a cup), inorganic resistors fabricated  
48  
49  
50 onto PVA substrate and the devices transferred onto an edge of the cup, respectively.  
51  
52

53  
54 Different technologies based on the concept of water assisted transfer can be used to  
55  
56  
57  
58  
59  
60

1  
2  
3 provide a conformal wrapping of devices onto an object. All benefit from water to partially  
4  
5  
6  
7 or fully dissolve the hydrosoluble substrate to transfer the devices. They are named tattoo  
8  
9  
10 electronics,<sup>35-37</sup> water transfer printing,<sup>6,38,39</sup> hydroprinting, etc.<sup>40</sup> Furthermore, previous  
11  
12  
13 works have demonstrated that the water transfer printing is a convenient technology to  
14  
15  
16  
17 fabricate large area electronics answering industrial issues.<sup>41</sup>  
18  
19  
20  
21

22 In this work, the external part of the cup has been humidify and the PVA substrate has  
23  
24  
25 been stuck to the external wall of the cup. Consequently, has already shown by Rogers  
26  
27  
28 et al. the bottom face of the PVA substrate is partially dissolved and conformably adheres  
29  
30  
31 to the object.<sup>42</sup> The figure 3d highlights that the resistive temperature sensor is still  
32  
33  
34  
35 working after it conformal mounting on the cup. One can notice that the value of the  
36  
37  
38 resistance equals 47.2 KOhm that is in the same range than for the experiments in the  
39  
40  
41 figure 2. This step can be considered as the testing step of a smart daily life object.  
42  
43  
44  
45

46 The figure 3e shows the evolution of the temperature inside (black curve) and in the external part  
47  
48 of the cup wall (red curve) when the cup is filled with boiling water and cool down. The  
49  
50 temperature inside and outside the wall has been measured using a k-probe thermocouple and an  
51  
52 IR-thermometer, respectively. As expected, the two temperatures follow the same trend, and the  
53  
54 temperature on the external part of the wall is systematically lower than the temperature inside.  
55  
56  
57  
58  
59  
60

1  
2  
3 Furthermore, when the cup is filled with boiling water, the temperature inside the cup grows up  
4 faster than this on the external part of the wall cup as also expected. The blue curve shows the  
5 variation of the sensor resistivity as function of the temperature. The trend of the blue curve follows  
6 the same behavior than the temperature measured using the IR-thermometer showing that the  
7 temperature at the surface of a daily life object can be monitored. The figure 3f highlights the  
8 dissolution of PVA when the cup is dipped into the water. It highlights the dismantling of the  
9 inorganic layer from the object. Indeed, as shown in the figure 3f, the PVA is fully dissolved after  
10 150 seconds detaching the inorganic devices. Thus, the object and the inorganic materials (after  
11 water filtration) can be recovered to be reused as shown in the figures 3g and 3h, respectively. At  
12 this step, two alternative can be chosen: object and inorganic materials can be recycled (second  
13 life) or destroyed following the WEEE standards. In both cases, this smart object end of life will  
14 be improved thanks to the eco-designed technology developed in this work. Moreover, even if  
15 silicon based materials remains in water, such inorganic nanomembrane will be fully dissolved as  
16 already reported in literature.<sup>43,44</sup>

### 35 **3. Conclusion**

36 Due to harmful aspects of human activity, our Mother Earth is facing environmental concerns.  
37 Plastic pollution is one of these environmental issues and the new generation of electronics that  
38 will flexible, stretchable, etc. have to take into consideration these issues. Here, a technologies  
39 allowing to wrap inorganic devices onto 3D object is reported. In addition to save electrical and  
40 mechanical capabilities, devices performed onto water soluble substrate can be dismantled from  
41 the object and recovered. Furthermore, it can be anticipated that other eco-friendly materials that  
42 can be put into solution can be compatible with the process described in this works.

## 4. Experimental Section

### a. Characterization:

Top-view images were obtained by PENTAX K70D equipped with a ZOOM macro 50mm (Pentax). Static I(V) electrical characteristics of the devices were collected at room temperature using an Agilent B1500A semiconductor parameter analyzer. Temperature were measured using a Fluke 51 II thermometer using an K-probe (Ohmega) and a Fluke 62 Max IR-thermometer.

### b. Fabrication

*PDMS adhesion layer:* Sylgard 184 PDMS was purchased from Dow Corning (Midland, U.S.A.), mixed with curing agent at a mass ratio of 10:1, and degassed for 30 min before spin-coating. Spin-coating parameters (velocity = 300 rpm; acceleration = 50 rpm.s<sup>-1</sup>; duration = 60 s) were kept constant for all the experiments (i.e., after curing, such spin-coating parameters allow the fabrication of 300µm thick PDMS on silicon substrates).

1  
2  
3  
4 Polyimide Substrate: A 25 $\mu\text{m}$  thick substrate of PI (DuPont<sup>TM</sup> France) were manually  
5  
6  
7 laminated onto the PDMS. Air bubbles trapped between PI and PDMS were removed  
8  
9  
10 under vacuum.

11  
12  
13  
14  
15 *PVA processing:* a PVA solution (PVA; Mw 9000-10000, 80% hydrolyzed from Aldrich)  
16  
17  
18 was prepared by mixing DI (deionized) water and PVA powder (5:1 w/w water/PVA) and  
19  
20  
21 filtering it with a 0.4  $\mu\text{m}$  filter. The PVA is filtered to avoid any aggregates. This step allows  
22  
23  
24 the fabrication of a PVA surfaces as smooth as possible (nanometric scale).PVA was  
25  
26  
27 spin-coated on PI substrates to form a 30- $\mu\text{m}$ -thick layer and baked at 100 $^{\circ}\text{C}$  for 2 hours.  
28  
29  
30  
31  
32 The spin-coating was performed at low rotation velocity 20 rpm and acceleration 10 rpm  
33  
34  
35 s<sup>-1</sup> for uniform thickness.  
36  
37

38  
39  
40 *Inorganic Thin film patterning:* A 150-nm-thick aluminum film was deposited by thermal  
41  
42  
43 evaporation at a deposition rate of 0.2 nm s<sup>-1</sup>. A classical lithographic process using  
44  
45  
46 S1818 (Dow electronic material MICROPOSIT) as photoresist (velocity = 4500 rpm;  
47  
48  
49 acceleration =5000 rpm s<sup>-1</sup>; duration = 60 s ) was performed to pattern the aluminum  
50  
51  
52  
53  
54 electrodes that can be both wet etched (H<sub>3</sub>PO<sub>4</sub>) or dry etched in ICP/RIE (inductive  
55  
56  
57  
58  
59  
60

1  
2  
3 coupled plasma / reactive ion etching) equipment from Corial (France) with the  
4  
5  
6  
7 experimental settings of 5 mTorr working pressure, 100 W plasma power, and chlorinated  
8  
9  
10 gas flow of 30 sccm.

11  
12  
13  
14 A 150-nm-thick silicon film was deposited by PECVD (Plasma Enhanced Chemical Vapor  
15  
16  
17  
18 Deposition. Experimental settings were adjusted as follows: The gazes' flow rate are fixed  
19  
20  
21  
22 to 1.5sccm of SiH<sub>4</sub>, 75sccm of H<sub>2</sub> and 75sccm of Ar (1% dilution of SiH<sub>4</sub> in Ar-H<sub>2</sub>  
23  
24  
25 mixture), 10Sccm of AsH<sub>3</sub>. The working pressure, the power and the temperature equals  
26  
27  
28 0.9mbar, 15W and 165°C, respectively. 1.8 μm thick of S1818 was spin-coated (velocity  
29  
30  
31 = 4500 rpm; acceleration =5000 rpm s<sup>-1</sup>; duration = 60s ) and used as mask to define  
32  
33  
34 the active area of the resistors. The n-doped Silicon was etched using SF<sub>6</sub> plasma (Roth  
35  
36 and Roh equipment). The experimental parameters were adjusted as follows: The gaze  
37  
38  
39 flow rate is fixed to 50sccm of SiH<sub>4</sub>. The working pressure, the power and the temperature  
40  
41  
42  
43 equals 30mTorr, 50W and 20°C, respectively.  
44  
45  
46  
47  
48  
49

50 *PI substrate etching:* dry etched in ICP/RIE (Corial, France) with the experimental settings  
51  
52  
53  
54 of 20 mTorr working pressure, 950 W and 50W for the ICP plasma and the RF power  
55  
56  
57  
58  
59  
60

1  
2  
3 respectively, an oxygen and Argon gases flow of 30 sccm 50 sccm respectively was used  
4  
5  
6  
7 to etch the PI film.  
8  
9  
10  
11  
12  
13  
14

### 15 **Acknowledgments**

16  
17  
18 This work is supported by the European Union through the European Regional  
19  
20  
21 Development Fund (ERDF), by the French region of Brittany (project: IMPRIM'), and by  
22  
23  
24  
25 IETR (project: 3DELEC).  
26  
27  
28  
29  
30  
31  
32  
33  
34  
35  
36  
37  
38  
39  
40  
41  
42  
43  
44  
45  
46  
47  
48  
49  
50  
51  
52  
53  
54  
55  
56  
57  
58  
59  
60

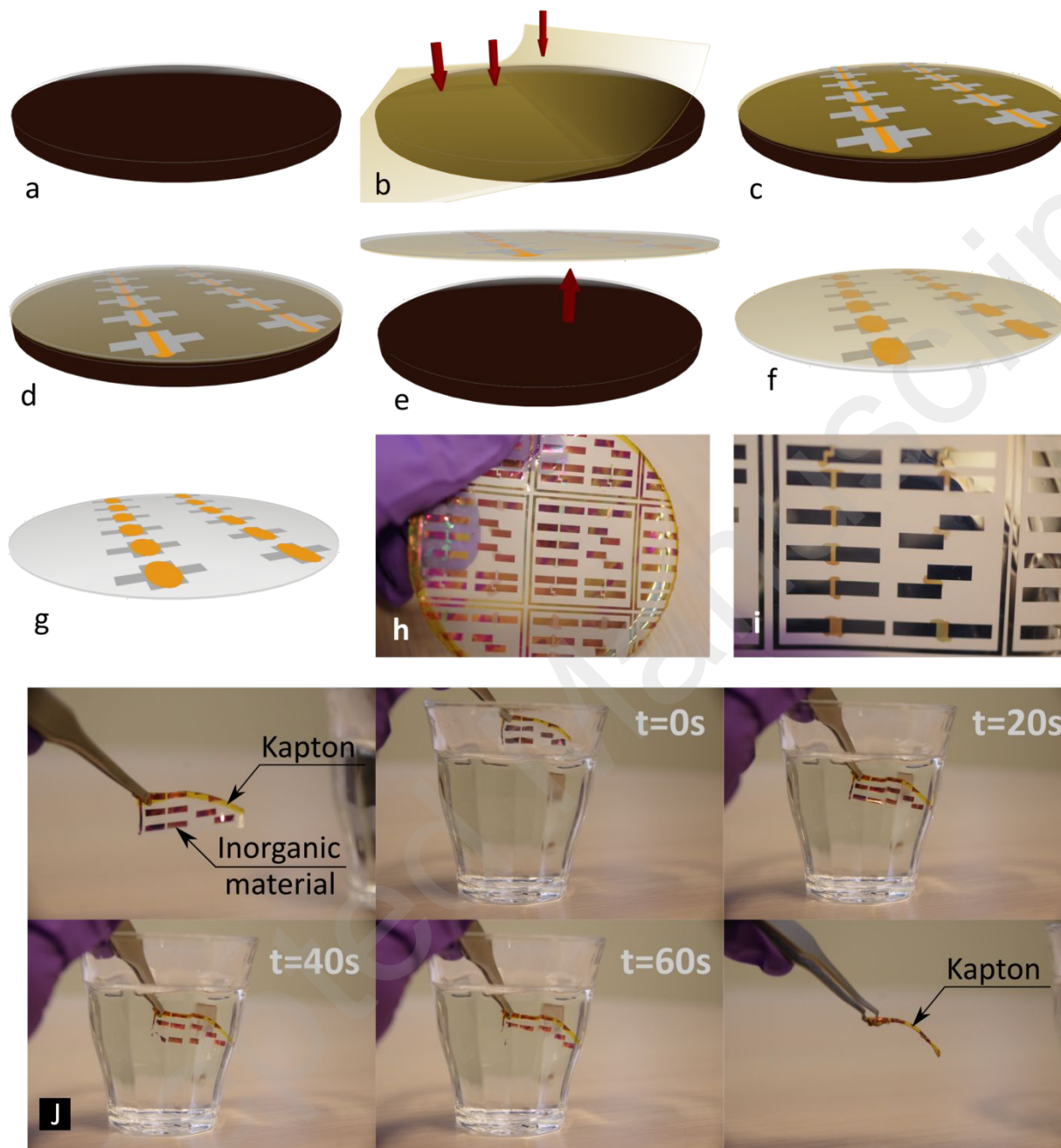
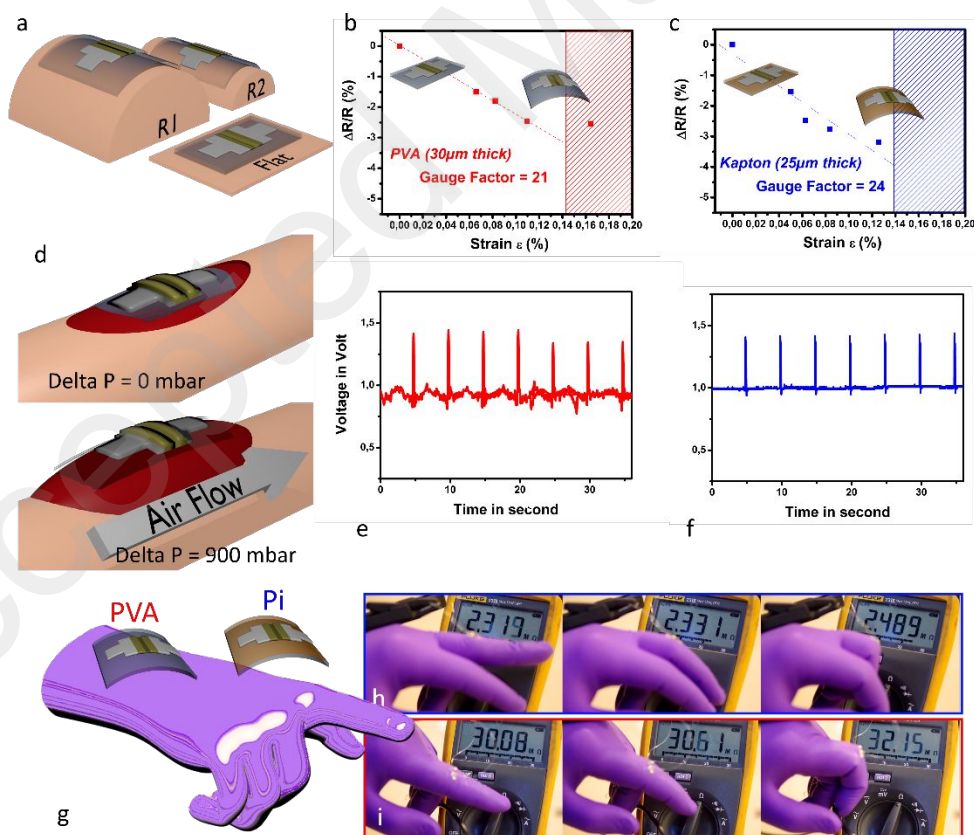


**Figure 1.** Inorganics multilayered electronics transferred onto PVA substrates. a) PDMS spincoated onto silicon substrate, b) PI substrate laminated onto PDMS, c) multilayered inorganic thin films patterned onto PI, d) PVA spin coating, e) PI substrates peeling from



1  
2  
3 the PDMS adhesive layer, f) Multilayered inorganic devices sandwiched between the PI  
4 and the PVA films, g) Inorganics devices transferred to the PVA substrates after dry  
5 etching of the PI substrate, h) optical picture after the PI etching; i) zoom in the devices;  
6  
7 and the PVA films, g) Inorganics devices transferred to the PVA substrates after dry  
8 etching of the PI substrate, h) optical picture after the PI etching; i) zoom in the devices;  
9  
10  
11  
12  
13  
14 j) Dissolution of the PVA substrate as function of time; To evaluate quantitatively the  
15 dissolution rate of PVA as function of additional external physical parameters such as  
16  
17  
18  
19  
20  
21  
22  
23  
24  
25  
26  
27  
28  
29  
30  
31  
32  
33  
34  
35  
36  
37  
38  
39  
40  
41  
42  
43  
44  
45  
46  
47  
48  
49  
50  
51  
52  
53  
54  
55  
56  
57  
58  
59  
60



1  
2  
3  
4  
5  
6 **Figure 2: Mechanical behavior of inorganic strain sensor fabricated onto PVA and**  
7  
8  
9 **Polyimide.** a) 3D view of the measurement protocol in static operating mode. For both  
10 technologies (PVA and Pi), the current versus the voltage is measured varying the radius  
11 of curvature (flat, 5cm, 2cm, 1.5cm and 1cm); The variation of the resistivity as function  
12 of applied strain for strain sensors fabricated onto: b) PI substrate and c) PVA substrate.  
13  
14  
15  
16  
17  
18  
19  
20  
21  
22  
23 d) 3D view of the measurement protocol in dynamic operating mode; The strain sensors  
24 is mounted onto a rubber membrane deformed by a differential of pressure (900mbar);  
25  
26  
27 For both technologies (PVA and Pi) response of voltage versus time at two different  
28 differential pressures (0 and 900mbar) for strain sensors fabricated onto : e) PI substrate  
29  
30  
31  
32  
33  
34  
35  
36  
37 and f) PVA substrate. g) 3D view of strain sensors (PVA and PI substrates) mounted onto  
38 a nitrile glove. Resistivity response varying the finger bending angle for sensors fabricated  
39  
40  
41  
42  
43  
44  
45 onto: h) the PVA substrate and i) the PI substrate.  
46  
47  
48  
49  
50  
51  
52  
53  
54  
55  
56  
57  
58  
59  
60

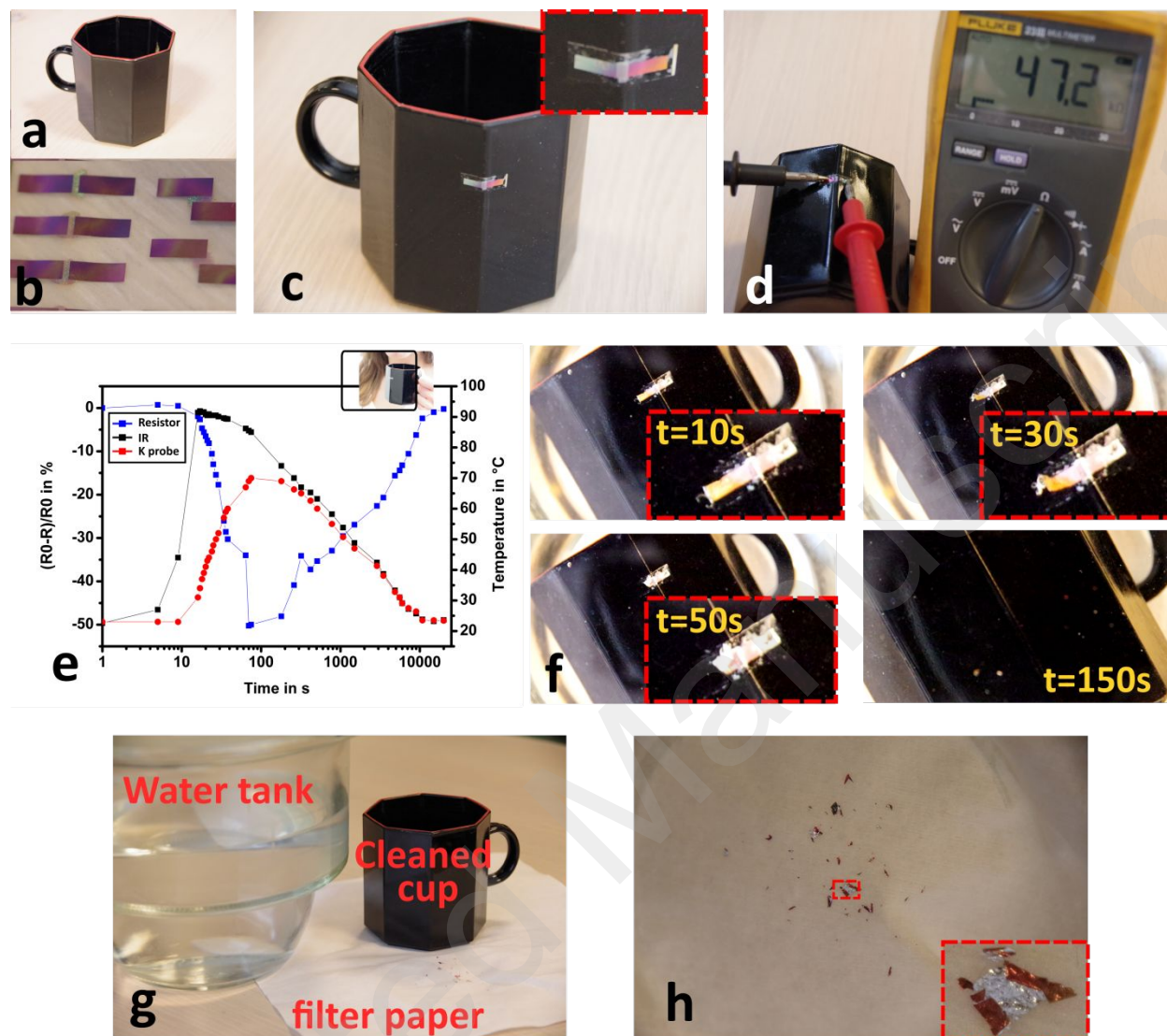


**Figure 3: Ecodesigned inorganic sensor fabricated onto PVA: dissolution, transfer, dismantling and recovery.** a) a cup as daily life object; b) resistor as temperature sensors fabricated onto PVA; c) water assisted transfer of the temperature sensors onto the cup. The inset highlights the inorganic device wraps onto a edge of the cup (angle =155°); d) electrical test of the resistor; e) Evolution of: i) the sensor resistivity as function of the cup

1  
2  
3 temperature (blue curves, left axe), ii) k-probe thermocouple (red curve, right axe), iii) IR  
4  
5  
6  
7 thermometer (black curve, right axe); f) dismantling of the inorganic device from the cup:  
8  
9  
10 g) The cup after dismantling the inorganic devices; h) inorganic films after filtration. The  
11  
12  
13  
14 inset highlights metal and silicon.  
15  
16  
17  
18  
19  
20  
21  
22  
23  
24  
25  
26  
27  
28  
29  
30  
31  
32  
33  
34  
35  
36  
37  
38  
39  
40  
41  
42  
43  
44  
45  
46  
47  
48  
49  
50  
51  
52  
53  
54  
55  
56  
57  
58  
59  
60

1  
2  
3  
4  
5  
6  
7  
8  
9  
10  
11  
12  
13  
14 ASSOCIATED CONTENT:  
15

16  
17 **Supporting information:**  
18

19  
20  
21 Table S1: Mechanical characteristics of inorganic material that constitute the strain  
22  
23  
24 sensor  
25

26  
27  
28 Figure S1: Optical picture of cracks in silicon thin films due to an excess of strain.  
29

30  
31 Figure S2: Setup used to deform and acquire the strain sensor electrical signal.  
32  
33

34  
35  
36  
37  
38 AUTHOR INFORMATION  
39

40  
41  
42 **Corresponding Author**  
43

44  
45  
46 Dr. M. Harnois,  
47  
48  
49  
50  
51  
52  
53  
54  
55  
56  
57  
58  
59  
60

1  
2  
3  
4 Université Rennes 1, Institut d'Électronique et des Télécommunications de Rennes,  
5  
6  
7 UMR CNRS 6164, Département Microélectronique & Microcapteurs, Campus de  
8  
9  
10 Beaulieu, 35042 Rennes Cedex, France.

11  
12  
13  
14  
15 E-mail : maxime.harnois@univ-rennes1.fr  
16  
17  
18  
19  
20  
21  
22  
23

#### 24 **Author Contributions**

25  
26  
27 The manuscript was written through contributions of all authors. All authors have given  
28  
29  
30 approval to the final version of the manuscript.  
31  
32  
33  
34

#### 35 **ACKNOWLEDGMENT**

36  
37  
38  
39 This work is supported by the European Union through the European Regional  
40  
41  
42 Development Fund (ERDF), by the French region of Brittany (project: IMPRIM'), and by  
43  
44  
45 IETR (project: 3DELEC).  
46  
47  
48  
49  
50  
51  
52  
53  
54  
55  
56  
57  
58  
59  
60

## References

- (1) Bohn, J.; Coroamă, V.; Langheinrich, M.; Mattern, F.; Rohs, M. Living in a World of Smart Everyday Objects—Social, Economic, and Ethical Implications. *Hum. Ecol. Risk Assess.* **2004**, *10* (5), 763–785.
- (2) Kibert, N. C. Extended Producer Responsibility: A Tool for Achieving Sustainable Development. *J. Land Use Environ. Law* **2004**, *19* (2), 503–523.
- (3) Goodship, V.; Stevels, A. *Waste Electrical and Electronic Equipment (WEEE) Handbook*; Elsevier, 2012.
- (4) Ongondo, F. O.; Williams, I. D.; Cherrett, T. J. How Are WEEE Doing? A Global Review of the Management of Electrical and Electronic Wastes. *Waste Manag.* **2011**, *31* (4), 714–730.
- (5) Khosla, A.; Ahmed, K.; Shiblee, M. N. I.; Thundat, T.; Nagahara, L. A.; Furukawa, H. Shape Conformable Flexible Sensors for Internet of Things (IoT): A Perspective. In *Meeting Abstracts*; The Electrochemical Society, 2018; pp 284–284.
- (6) Le Borgne, B.; De Sagazan, O.; Crand, S.; Jacques, E.; Harnois, M. Conformal Electronics Wrapped Around Daily Life Objects Using an Original Method: Water Transfer Printing. *ACS Appl. Mater. Interfaces* **2017**, *9* (35), 29424–29429.
- (7) Zhang, Z.; Cui, L.; Shi, X.; Tian, X.; Wang, D.; Gu, C.; Chen, E.; Cheng, X.; Xu, Y.; Hu, Y.; J. Zhang; L. Zhou; H.H. Fong; P. Ma; G. Jiang; X. Sun; B. Zhang; H. Peng; Textile Display for Electronic and Brain-Interfaced Communications. *Adv. Mater.* **2018**, *30* (18), 1800323.
- (8) Sekitani, T.; Nakajima, H.; Maeda, H.; Fukushima, T.; Aida, T.; Hata, K.; Someya, T. Stretchable Active-Matrix Organic Light-Emitting Diode Display Using Printable Elastic Conductors. *Nat. Mater.* **2009**, *8* (6),
- (9) Kaltenbrunner, M.; White, M. S.; Głowacki, E. D.; Sekitani, T.; Someya, T.; Sariciftci, N. S.; Bauer, S. Ultrathin and Lightweight Organic Solar Cells with High Flexibility. *Nat. Commun.* **2012**, *3*, 770.

- 1  
2  
3  
4 (10) Peng, X.; Yuan, J.; Shen, S.; Gao, M.; Chesman, A. S.; Yin, H.; Cheng, J.; Zhang,  
5 Q.; Angmo, D. Perovskite and Organic Solar Cells Fabricated by Inkjet Printing:  
6 Progress and Prospects. *Adv. Funct. Mater.* **2017**, *27*(41), 1703704.  
7  
8 (11) Adams, J. J.; Duoss, E. B.; Malkowski, T. F.; Motala, M. J.; Ahn, B. Y.; Nuzzo, R.  
9 G.; Bernhard, J. T.; Lewis, J. A. Conformal Printing of Electrically Small Antennas  
10 on Three-Dimensional Surfaces. *Adv. Mater.* **2011**, *23*(11), 1335–1340.  
11  
12 (12) Kraus, J. D.; Marhefka, R. J. Antennas for All Applications. *Antennas Appl. Kraus*  
13 *John Daniel Marhefka Ronald J N. Y. McGraw-Hill C2002 2002*.  
14  
15 (13) Salvatore, G. A.; Münzenrieder, N.; Kinkeldei, T.; Petti, L.; Zysset, C.; Strebel, I.;  
16 Büthe, L.; Tröster, G. Wafer-Scale Design of Lightweight and Transparent  
17 Electronics That Wraps around Hairs. *Nat. Commun.* **2014**, *5*, 2982.  
18  
19 (14) Rogers, J. A.; Someya, T.; Huang, Y. Materials and Mechanics for Stretchable  
20 Electronics. *Science* **2010**, *327*(5973), 1603–1607.  
21  
22 (15) Zhang, Y.; Xu, S.; Fu, H.; Lee, J.; Su, J.; Hwang, K.-C.; Rogers, J. A.; Huang, Y.  
23 Buckling in Serpentine Microstructures and Applications in Elastomer-Supported  
24 Ultra-Stretchable Electronics with High Areal Coverage. *Soft Matter* **2013**, *9*(33),  
25 8062.  
26  
27 (16) Kim, D.-H.; Lu, N.; Ma, R.; Kim, Y.-S.; Kim, R.-H.; Wang, S.; Wu, J.; Won, S. M.;  
28 Tao, H.; Islam, A.; Yu, K. J.; Kim, T.-I.; Chowdhury, R.; Ying, M.; Xu, L.; Li M.; Chung,  
29 H. J.; Keum, H.; McCormick, M.; Liu, P.; Zhang, Y-W; Omenetto, F. G.; Huan, Y.;  
30 Coleman, T.; Rogers, J. A. Epidermal Electronics. *science* **2011**, *333*(6044), 838–  
31 843.  
32  
33 (17) Rogel, R.; Borgne, B. L.; Mohammed-Brahim, T.; Jacques, E.; Harnois, M.  
34 Spontaneous Buckling of Multiaxially Flexible and Stretchable Interconnects Using  
35 PDMS/Fibrous Composite Substrates. *Adv. Mater. Interfaces* **2017**, *4*(3), 1600946.  
36  
37 (18) Yang, Y.; Vervust, T.; Dunphy, S.; Van Put, S.; Vandecasteele, B.; Dhaenens, K.;  
38 Degrendele, L.; Mader, L.; De Vriese, L.; Martens, T.; Kaufmann, M.; Sekitani, T.;  
39 Vanfleteren, J.. 3D Multifunctional Composites Based on Large-Area Stretchable  
40 Circuit with Thermoforming Technology. *Adv. Electron. Mater.* **2018**, 1800071.  
41  
42 (19) Irimia-Vladu, M. “Green” Electronics: Biodegradable and Biocompatible Materials  
43 and Devices for Sustainable Future. *Chem. Soc. Rev.* **2014**, *43*(2), 588–610.  
44  
45  
46  
47  
48  
49  
50  
51  
52  
53  
54  
55  
56  
57  
58  
59  
60

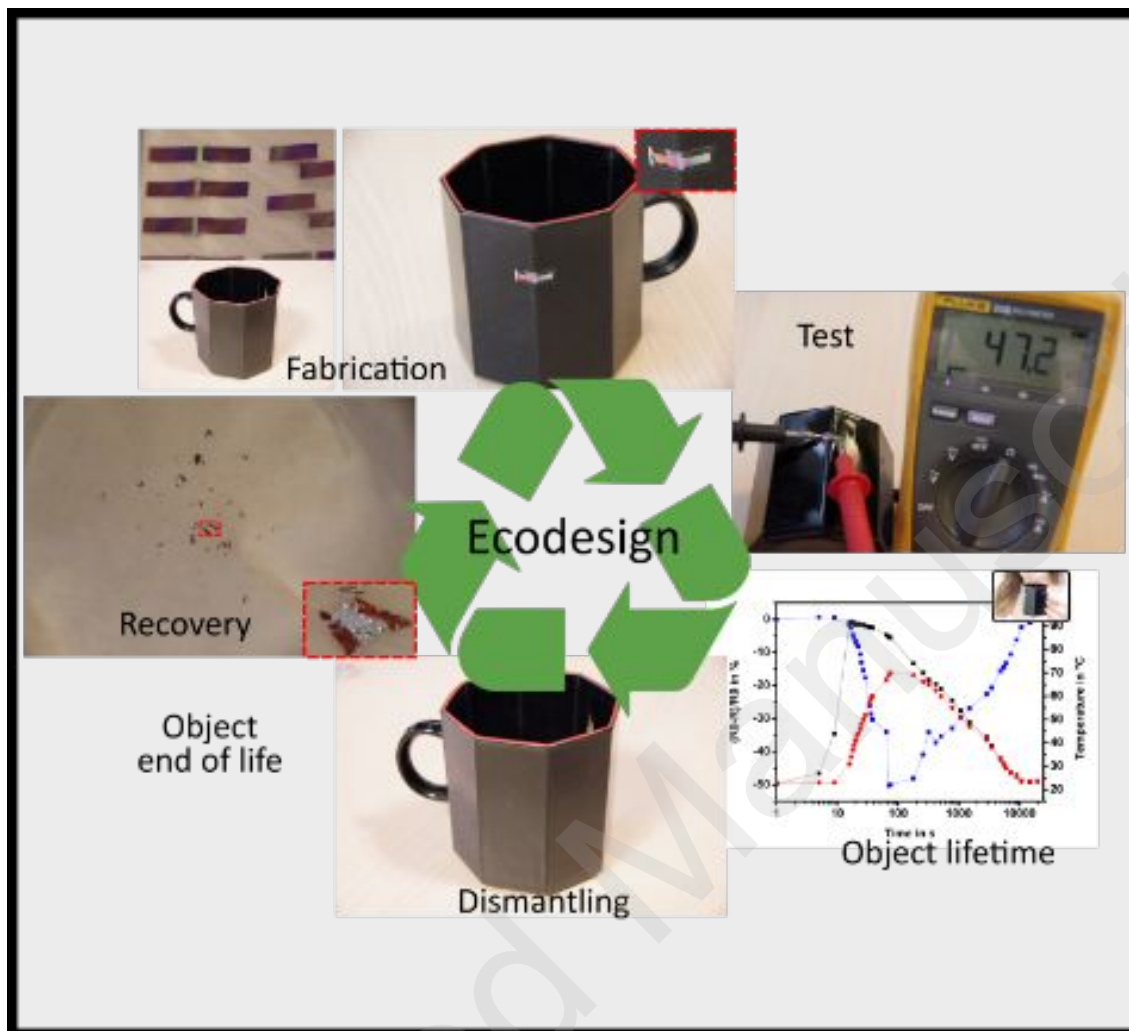


- 1  
2  
3  
4 (20) Irimia-Vladu, M.; Glowacki, E. D.; Voss, G.; Bauer, S.; Sariciftci, N. S. Green and  
5 Biodegradable Electronics. *Mater. Today* **2012**, *15*(7–8), 340–346.  
6  
7 (21) Le Borgne, B.; Chung, B.-Y.; Tas, M. O.; King, S. G.; Harnois, M.; Sporea, R. A.  
8 Eco-Friendly Materials for Daily-Life Inexpensive Printed Passive Devices: Towards  
9 “Do-It-Yourself” Electronics. *Electronics* **2019**, *8*(6), 699.  
10  
11 (22) Moorthy, B.; Baek, C.; Wang, J. E.; Jeong, C. K.; Moon, S.; Park, K.-I.; Kim, D. K.  
12 Piezoelectric Energy Harvesting from a PMN–PT Single Nanowire. *RSC Adv.* **2017**,  
13 *7*(1), 260–265.  
14  
15 (23) Zhang, Y.; Sun, H.; Jeong, C. K. Biomimetic Porifera Skeletal Structure of Lead-  
16 Free Piezocomposite Energy Harvesters. *ACS Appl. Mater. Interfaces* **2018**, *10*  
17 (41), 35539–35546.  
18  
19 (24) Li, R.; Wang, L.; Kong, D.; Yin, L. Recent Progress on Biodegradable Materials and  
20 Transient Electronics. *Bioact. Mater.* **2018**, *3*(3), 322–333.  
21  
22 (25) Fodil, K.; Denoual, M.; Dolabdjian, C.; Harnois, M.; Senez, V. Dynamic Sensing of  
23 Magnetic Nanoparticles in Microchannel Using GMI Technology. *IEEE Trans.*  
24 *Magn.* **2012**, *49*(1), 93–96.  
25  
26 (26) Yang, S.; Lu, N. Gauge Factor and Stretchability of Silicon-on-Polymer Strain  
27 Gauges. *Sensors* **2013**, *13*(7), 8577–8594.  
28  
29 (27) French, P.; Evans, A. Piezoresistance in Polysilicon and Its Applications to Strain  
30 Gauges. *Solid-State Electron.* **1989**, *32*(1), 1–10.  
31  
32 (28) Gleskova, H.; Wagner, S.; Soboyejo, W.; Suo, Z. Electrical Response of  
33 Amorphous Silicon Thin-Film Transistors under Mechanical Strain. *J. Appl. Phys.*  
34 **2002**, *92*(10), 6224–6229.  
35  
36 (29) Kervran, Y.; De Sagazan, O.; Crand, S.; Coulon, N.; Mohammed-Brahim, T.; Brel,  
37 O. Microcrystalline Silicon: Strain Gauge and Sensor Arrays on Flexible Substrate  
38 for the Measurement of High Deformations. *Sens. Actuators Phys.* **2015**, *236*, 273–  
39 280.  
40  
41 (30) Faurie, D.; Renault, P.-O.; Le Bourhis, E.; Villain, P.; Goudeau, P.; Badawi, F.  
42 Measurement of Thin Film Elastic Constants by X-Ray Diffraction. *Thin Solid Films*  
43 **2004**, *469*, 201–205.  
44  
45  
46  
47  
48  
49  
50  
51  
52  
53  
54  
55  
56  
57  
58  
59  
60

- 1  
2  
3  
4 (31) Kaltenbrunner, M.; Sekitani, T.; Reeder, J.; Yokota, T.; Kuribara, K.; Tokuhara, T.;  
5 Drack, M.; Schwödiauer, R.; Graz, I.; Bauer-Gogonea, S.; Bauer, S.; Someya, T.  
6 An Ultra-Lightweight Design for Imperceptible Plastic Electronics. *Nature* **2013**, *499*  
7 (7459), 458–463.  
8  
9  
10 (32) Chortos, A.; Liu, J.; Bao, Z. Pursuing Prosthetic Electronic Skin. *Nat. Mater.* **2016**,  
11 *15*(9), 937.  
12  
13 (33) Yang, S.; Chen, Y.-C.; Nicolini, L.; Pasupathy, P.; Sacks, J.; Su, B.; Yang, R.;  
14 Sanchez, D.; Chang, Y.-F.; Wang, P.; Schnyer, D.; Neikirk, D.; Lu, N. “Cut-and-  
15 Paste” Manufacture of Multiparametric Epidermal Sensor Systems. *Adv. Mater.*  
16 **2015**, *27*(41), 6423–6430.  
17  
18 (34) Martinho, G.; Pires, A.; Saraiva, L.; Ribeiro, R. Composition of Plastics from Waste  
19 Electrical and Electronic Equipment (WEEE) by Direct Sampling. *Waste Manag.*  
20 **2012**, *32*(6), 1213–1217.  
21  
22 (35) Wang, Y.; Qiu, Y.; Ameri, S. K.; Jang, H.; Dai, Z.; Huang, Y.; Lu, N. Low-Cost, Mm-  
23 Thick, Tape-Free Electronic Tattoo Sensors with Minimized Motion and Sweat  
24 Artifacts. *Npj Flex. Electron.* **2018**, *2*(1), 6.  
25  
26 (36) Kabiri Ameri, S.; Ho, R.; Jang, H.; Tao, L.; Wang, Y.; Wang, L.; Schnyer, D. M.;  
27 Akinwande, D.; Lu, N. Graphene Electronic Tattoo Sensors. *ACS Nano* **2017**, *11*  
28 (8), 7634–7641.  
29  
30 (37) Kim, D.-H.; Viventi, J.; Amsden, J. J.; Xiao, J.; Vigeland, L.; Kim, Y.-S.; Blanco, J.  
31 A.; Panilaitis, B.; Frechette, E. S.; Contreras, D.; Kaplan, D. L.; Omenetto F. G.;  
32 Huang Y.; Hwang, K. C.; Zakin, M. R.; Litt, B.; Rogers, J. A. Dissolvable Films of  
33 Silk Fibroin for Ultrathin Conformal Bio-Integrated Electronics. *Nat. Mater.* **2010**, *9*  
34 (6), 511–517.  
35  
36 (38) Le Borgne, B.; Jacques, E.; Harnois, M. The Use of a Water Soluble Flexible  
37 Substrate to Embed Electronics in Additively Manufactured Objects: From Tattoo to  
38 Water Transfer Printed Electronics. *Micromachines* **2018**, *9*(9), 474.  
39  
40 (39) Ng, L. W.; Zhu, X.; Hu, G.; Macadam, N.; Um, D.; Wu, T.-C.; Moal, F. L.; Jones, C.  
41 G.; Hasan, T. Conformal Printing of Graphene for Single and Multi-Layered Devices  
42 on to Arbitrarily Shaped 3D Surfaces. *ArXiv Prepr. ArXiv181101073* **2018**.  
43  
44  
45  
46  
47  
48  
49  
50  
51  
52  
53  
54  
55  
56  
57  
58  
59  
60

- 1  
2  
3  
4 (40) Saada, G.; Layani, M.; Chernevousky, A.; Magdassi, S. Hydroprinting Conductive  
5 Patterns onto 3D Structures. *Adv. Mater. Technol.* **2017**, *2* (5), 1600289.  
6  
7 (41) Le Borgne, B.; Liu, S.; Morvan, X.; Crand, S.; Sporea, R. A.; Lu, N.; Harnois, M.  
8 Water Transfer Printing Enhanced by Water-Induced Pattern Expansion: Toward  
9 Large-Area 3D Electronics. *Adv. Mater. Technol.* **2019**, 1800600.  
10  
11 (42) Tao, H.; Brenckle, M. A.; Yang, M.; Zhang, J.; Liu, M.; Siebert, S. M.; Averitt, R. D.;  
12 Mannoor, M. S.; McAlpine, M. C.; Rogers, J. A.; Kaplan, D. A.; Omenetto, F. G.  
13 Silk-Based Conformal, Adhesive, Edible Food Sensors. *Adv. Mater.* **2012**, *24* (8),  
14 1067–1072.  
15  
16 (43) Hwang, S.-W.; Park, G.; Edwards, C.; Corbin, E. A.; Kang, S.-K.; Cheng, H.; Song,  
17 J.-K.; Kim, J.-H.; Yu, S.; Ng, J.; Lee, J. E.; Kim, J.; Yee, C.; Bhaduri, B.; Su, Y.;  
18 Omenetto, F.G.; Huang, Y.; Bashir, R.; Goddard, L.; Popescu, G.; Lee, K.M.;  
19 Rogers, J. A. Dissolution Chemistry and Biocompatibility of Single-Crystalline  
20 Silicon Nanomembranes and Associated Materials for Transient Electronics. *ACS*  
21 *Nano* **2014**, *8* (6), 5843–5851.  
22  
23 (44) Kang, S.-K.; Hwang, S.-W.; Cheng, H.; Yu, S.; Kim, B. H.; Kim, J.-H.; Huang, Y.;  
24 Rogers, J. A. Dissolution Behaviors and Applications of Silicon Oxides and Nitrides  
25 in Transient Electronics. *Adv. Funct. Mater.* **2014**, *24* (28), 4427–4434.  
26  
27  
28  
29  
30  
31  
32  
33  
34  
35  
36  
37  
38  
39  
40  
41  
42  
43  
44  
45  
46  
47  
48  
49  
50  
51  
52  
53  
54  
55  
56  
57  
58  
59  
60

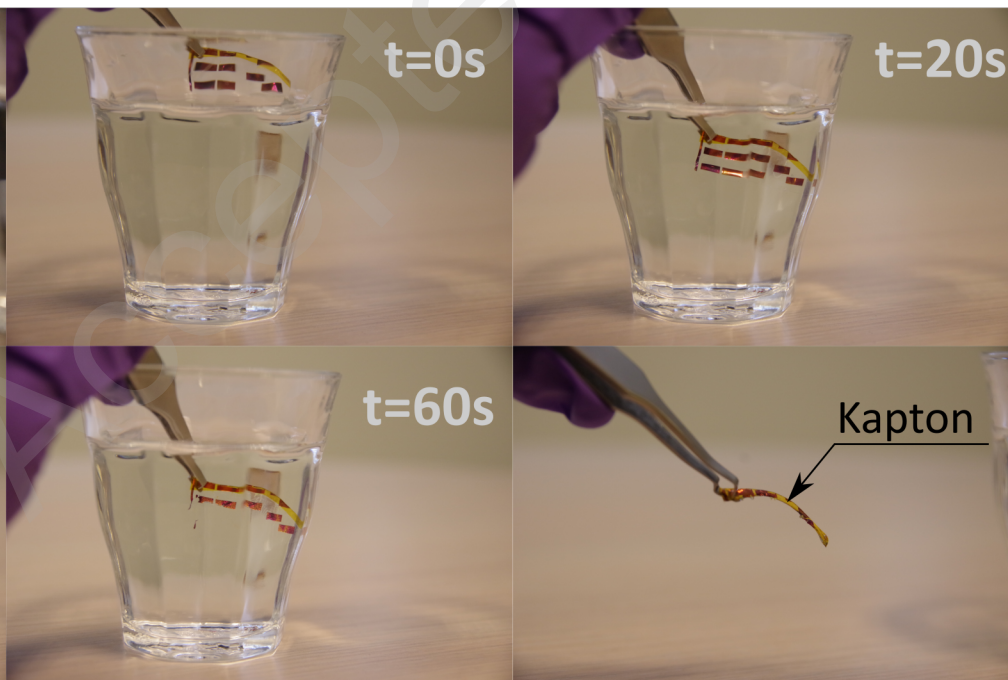
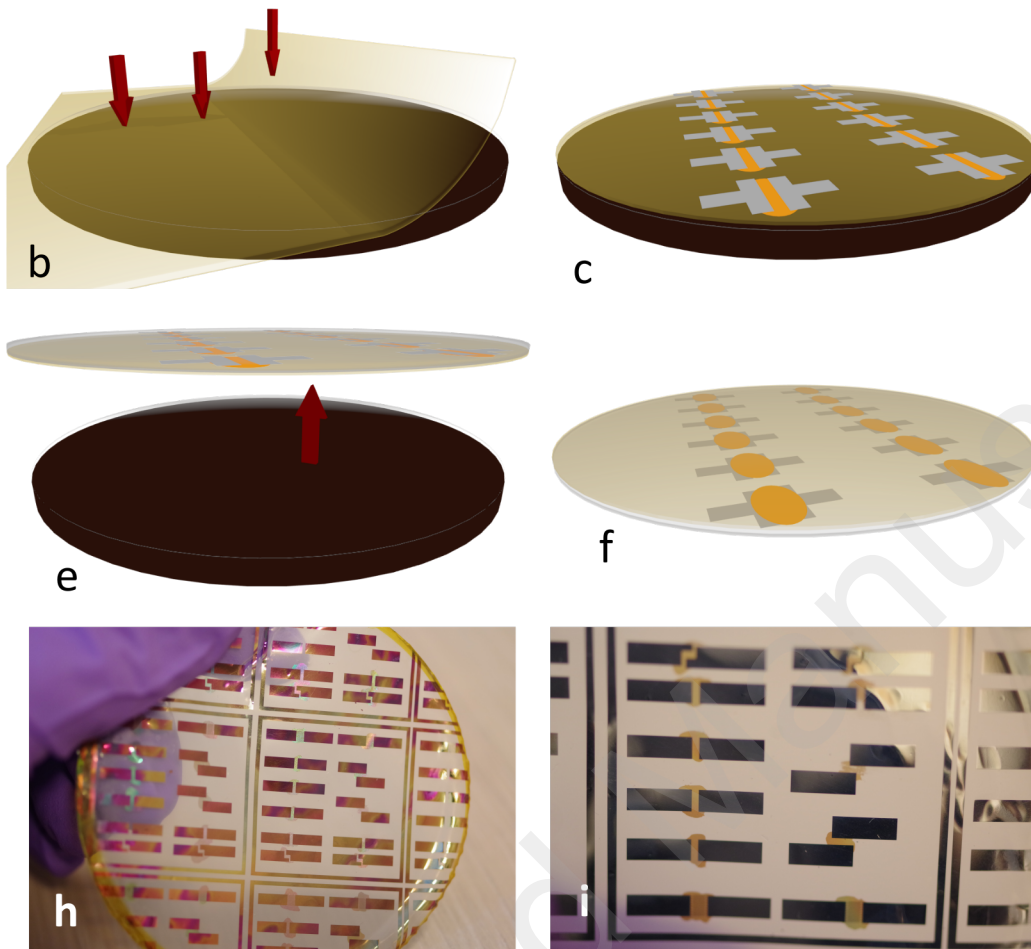
ToC figure

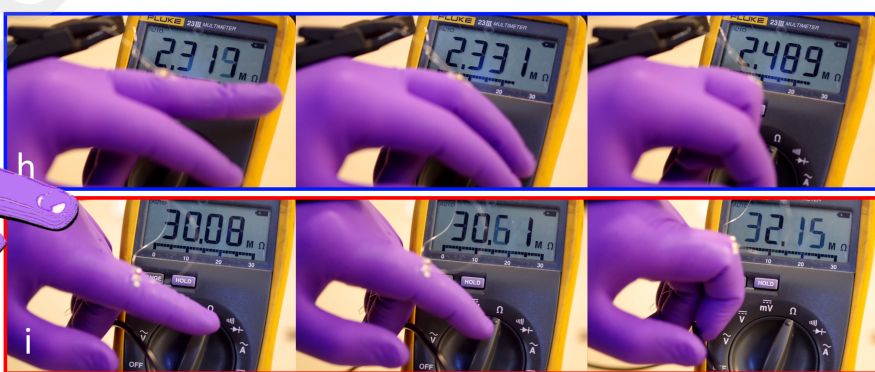
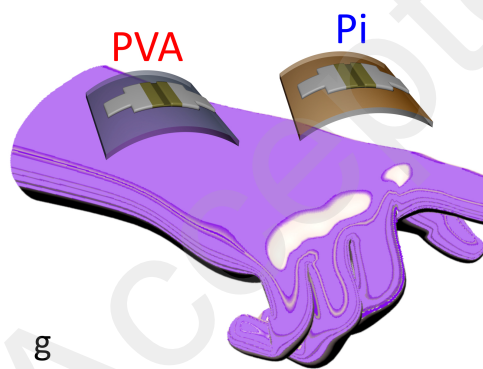
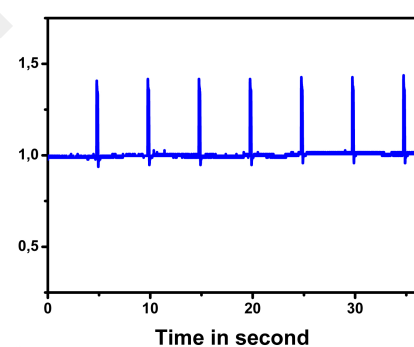
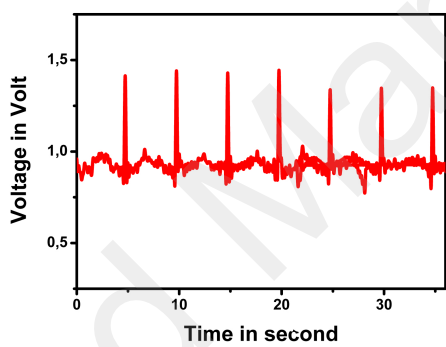
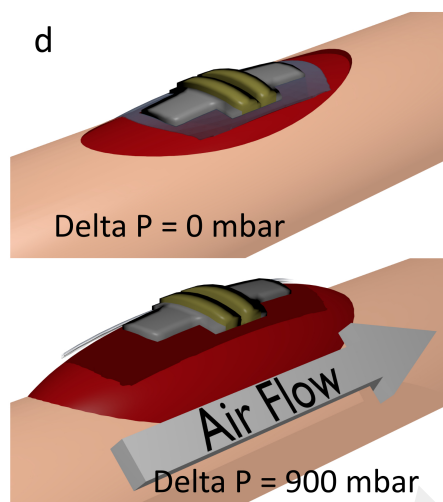
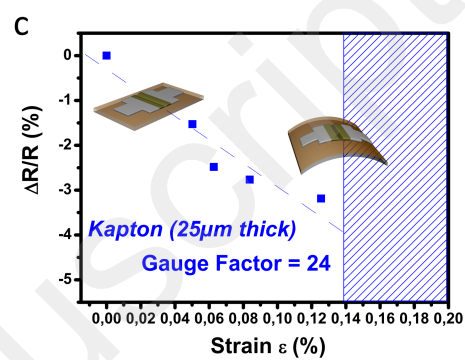
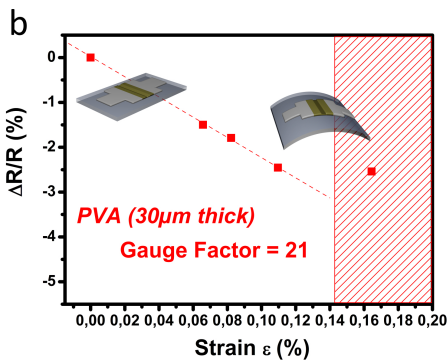
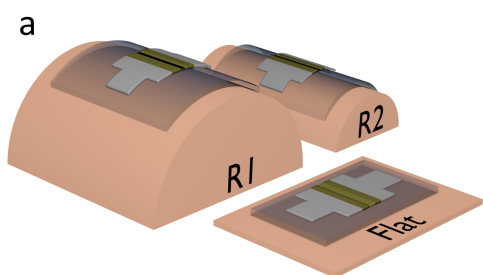


1  
2  
3  
4  
5  
6  
7  
8  
9  
10  
11  
12  
13  
14  
15  
16  
17  
18  
19  
20  
21  
22  
23  
24  
25  
26  
27  
28  
29  
30  
31  
32  
33  
34  
35  
36  
37  
38  
39  
40  
41  
42  
43  
44  
45  
46  
47  
48  
49  
50  
51  
52  
53  
54  
55  
56  
57  
58  
59  
60

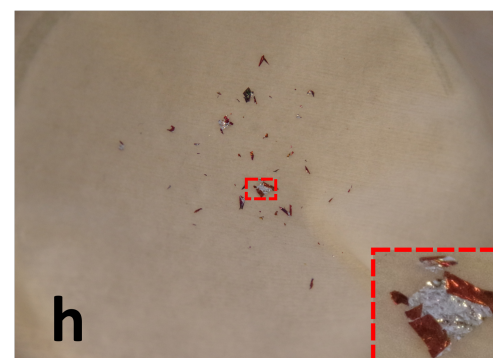
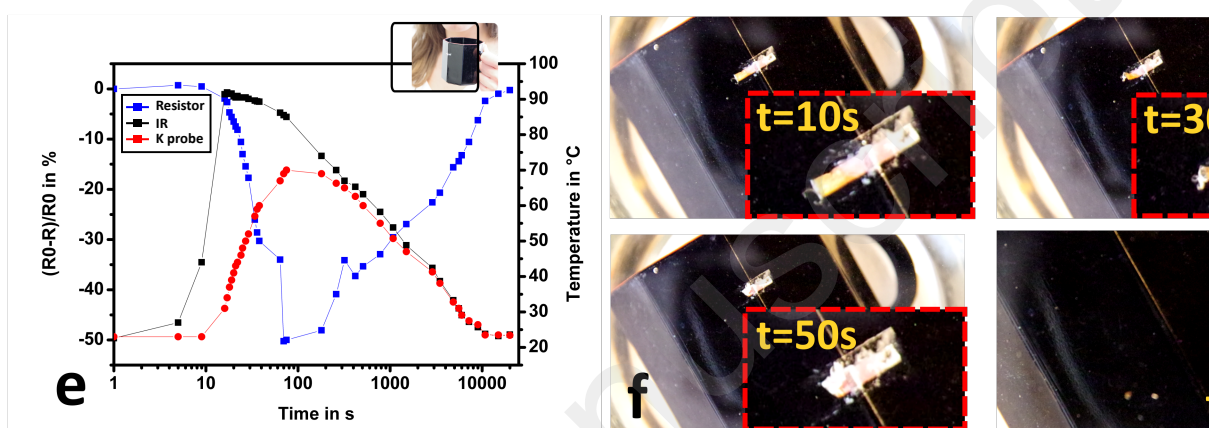
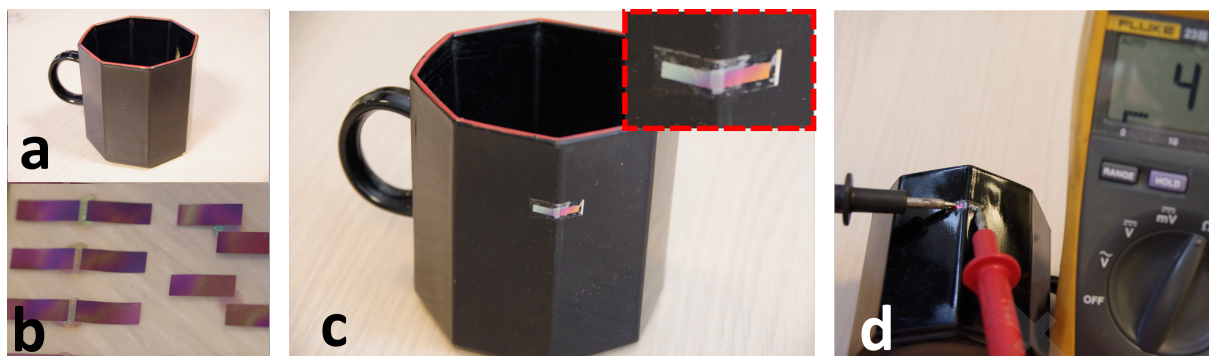
Accepted Manuscript

1  
2  
3  
4  
5  
6  
7  
8  
9  
10  
11  
12  
13  
14  
15  
16  
17  
18  
19  
20  
21  
22  
23  
24  
25  
26  
27  
28  
29  
30  
31  
32  
33  
34  
35  
36  
37  
38  
39  
40  
41  
42  
43  
44  
45  
46  
47  
48  
49  
50  
51  
52  
53  
54  
55  
56  
57  
58  
59  
60











1  
2  
3  
4  
5  
6  
7  
8  
9  
10  
11  
12  
13  
14  
15  
16  
17  
18  
19  
20  
21  
22  
23  
24  
25  
26  
27  
28  
29  
30  
31  
32  
33  
34  
35  
36  
37  
38  
39  
40  
41  
42  
43  
44  
45  
46  
47  
48  
49  
50  
51  
52  
53  
54  
55  
56  
57  
58  
59  
60

